Improving the width of lossy mode resonances in reflection configuration D-shaped fiber by nanocoating laser ablation

OMAR FUENTES,[1,2,*] PATRIZIO VAIANO,[3] IGNACIO DEL VILLAR,[1,4] GIUSEPPE QUERO,[3] JESÚS CORRES,[4] MARCO CONSALES,[3] IGNACIO MATÍAS,[1] ANDREA CUSANO[3]

[1]*Institute of Smart Cities, Public University of Navarre, 31006 Pamplona, Spain*
[2]*Department of Telecommunications and Electronics, Pinar del Río University, Pinar del Río, 20100, Cuba*
[3]*Optoelectronics Group, Department of Engineering, University of Sannio, I-82100, Benevento, Italy*
[4]*Department of Electrical and Electronic Engineering, Public University of Navarre, 31006 Pamplona, Spain*
**Corresponding author: omar.fuentes@unavarra.es*

Received XX Month XXXX; revised XX Month, XXXX; accepted XX Month XXXX; posted XX Month XXXX (Doc. ID XXXXX); published XX Month XXXX

Abstract

The full-width at half maximum (FWHM) of lossy mode resonances (LMRs) in the optical spectrum depends on the homogeneity of the thin-film deposited. Here, a method for improving the FWHM is applied for an LMR generated by a D-shaped optical fiber in reflection configuration. To this purpose, three samples with different attenuation were deposited with DC sputtering thin-films of SnO_{2-x} and a further controlled immersion in water of the samples was performed. A laser cleaner method was used to improve the FWHM characteristics of one of the samples from 106 nm to 53 nm. This improvement can be applied to thin-film based sensors where there is a problem of inhomogeneity of the coating thickness. Moreover, with this technique it was proved that a coated length of just 3-4 mm permits to generate an LMR, with what this imply in terms of miniaturization of the final device.

OCIS codes: *(060.2430) Fibers, single-mode (310.0310) Thin-films, (060.2370) Fiber optics sensors.*

Both surface plasmon resonances (SPRs) and lossy mode resonances (LMRs) are based on light coupling due to deposition of a thin-film on a dielectric medium [1-5]. LMRs present some properties that make them more versatile compared to SPRs: they can be obtained in a wide range of materials that include mainly metallic oxides and polymers [6-8], they can be excited both at TE and TM polarization, and multiple resonances in the same spectrum can be generated [4]. On the other hand, because it is obtained with incidence angles close to 90º, it has been widely used in multimode fibers and tapered fibers [9-13], and also recently by lateral incidence of light on the edge of a glass coverslip or a microscope slide [14].

Regarding optical fibers, one of the most widely used structures for generating LMRs is the D-shaped fiber in transmission [15, 16]. However, this configuration has the drawback that it is not as easy to handle as a fiber in the reflection configuration, which allows the device to be used as a catheter, [17, 18], a nasogastric probe [19], or even for chemical mapping of surfaces [20].

Another interesting property of LMRs is that their central wavelength is directly related to the coating thickness. Hence, it is easy to tune their position in a broadband spectral range [4]. This also explains their high sensitivity [3]. However, this versatility becomes a drawback when the thickness of the nanocoating along the fiber length is not uniform, which may occur due to the distance and inclination with which the sample is positioned inside the sputtering machine or to the parameters used for rotating the platform where the sample is placed on [21-23].

Here it will be demonstrated that it is possible to improve the full width at half maximum (FWHM) of the LMR, which is important for obtaining a high figure of merit, one of the main parameters used for assessing the performance of a refractometer and also a key parameter to determine the limit of detection in chemical sensors and biosensors [24]. Initially, this will be demonstrated by immersing different lengths of the device in water, whereas a more robust procedure based on laser ablation will be applied to confirm this idea.

In order to analyze this, three different D-shaped fiber samples from Phoenix Photonics Ltd (Kent, UK) were used: S1, S2 and S3. The D-shaped fibers consisted of a standard single mode fiber (SMF-28 from Corning) with a side-polished length of 10 mm. The attenuation of light transmitted through sample S1 was -0.3 dB in high index oil (refractive index 1.45), whereas the attenuation of samples S2 and S3 was -0.7 dB. In other words, the degree of polishing of samples S2 and S3 was higher than in samples S1 in order to compare the results obtained with two different degrees of polishing.

The samples were cleaved at a 90° angle after the polished region for a further deposition of a gold layer that guarantees that all light that reaches the tip of the fiber is reflected back. In this way, the performance of the reflection configuration D-shaped fiber must be the same as a transmission configuration D-shaped fiber but with the exception that light passes two times through the same polished region. In other words, a 10 mm long D-shaped fiber in reflection configuration should perform like a 20 mm long D-shaped fiber in transmission.

In order to guarantee the good adhesion of the 110 nm gold layer at the end of the fiber, a titanium layer of 10 nm was initially deposited. Both the titanium and the gold layer were deposited by means of an Electron beam evaporator (Kenosistec CL400C, Binasco (MI), Italy). To avoid the material deposition onto the lateral surface of the D-shaped fiber, the samples were inserted into a loose tube leaving only the end face of the optical fiber exposed to the evaporation process.

After the deposition of the mirror, the next step was to deposit a thin film on the surface of the optical fiber D-shaped zone using a DC sputtering machine (K675XD from Quorum Technologies, Ltd.) with a black tin oxide (SnO_{2-x}) target from Loyaltarget Technology Co. The deposition was monitored with a RIFOCS 575L power meter and Pyroistech COB-840 light source as depicted in Fig. 1. When the power from the light source reached a minimum, the deposition was stopped. This permitted to position the resonance at about 900 nm in air and 1600 nm in water.

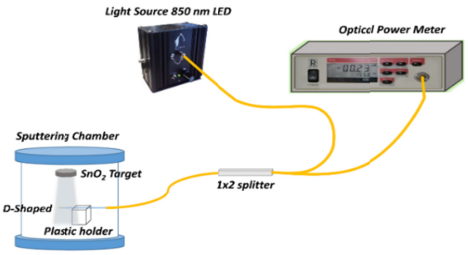

Fig 1: Experimental setup for deposition of D-shaped fibers in reflection configuration

Fig 2a shows a schematic of the D-shaped fiber in reflection configuration, where the different parts can be distinguished: the polished region (L1), the tapered regions (L2), the gold mirror region (L3) the distance from the tip to the polished region (L4) and the diameter of D-shaped (d), which is about 73 µm in the three samples. In Fig. 2b-d, photographs of samples S1, S2 and S3 are shown, where the values of the different regions can be observed in table 1. The reflected optical spectrum was monitored during the immersion of each D-shaped fiber in water. The setup consisted of several elements described in Fig. 3.

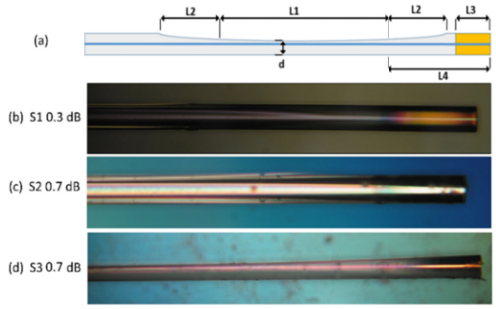

Fig 2: (a) Schematic of the fibers with the polished region (L1), the tapered regions (L2), the gold mirror region (L3) and the distance from the tip to the polished region (L4). (b-d) Photographs of samples S1, S2 and S3.

	L1 (mm)	L2 (mm)	L3 (mm)	L4 (mm)
S1	9.0	0.5	0.4	1.8
S2	9.0	0.6	0.4	1.05
S3	9.0	0.5	0.2	0.5

Table 1: Parameters of samples S1, S2 and S3.

A broadband light source (NKT SuperK COMPACT) was connected to end 1 of a single-mode fiber 2x2 splitter (the polarization state of light was controlled with a fiber-optic in-line polarizer and a polarization controller). The end 2 of the splitter was connected to the SMF pigtail with the D-shaped fiber, the end 3 was connected to an Optical Spectrum Analyzer (Yokogawa AQ6370D, OSA 1) used for monitoring the signal probe, and the end 4 was connected to another optical spectrum analyzer (Yokogawa AQ6370D, OSA 2) used for monitoring the reference signal.

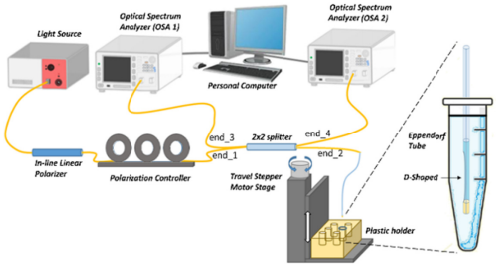

Fig 3: Experimental setup for monitoring the reflected optical spectrum when the fiber is immersed in water in steps of 1 mm.

Initially, the LMR was located at about 900nm in air. After that, the sample was immersed in water in steps of 1 mm, which led to the progressive generation of an LMR in the infrared for each sample analyzed: S1, S2 and S3 (see Fig. 4). For the first sample, S1 in Fig. 4(a), the LMR starts to be visible at 3 mm of immersion in water and at 5 mm the LMR reaches the maximum depth. After that, the resonance broadens and its shape progressively stabilizes until it is completely immersed in water. The effect of wetting in the properties of the material should be considered if the LMRs were due to both air and water immersed regions. However, in the operating wavelength range the LMR is due to the water immersed region (the first LMR in air is very separated [3]). Therefore, this effect of the refractive index difference between immersed and non-immersed regions is discarded. Another important question is the meniscus height., which according to [25] is 2 times de diameter of the fiber (2x80 micron=0.16 mm). Therefore, the effect is not negligible but less than the resolution of the measurement (0.16 mm vs 1 mm). The behavior of sample S2, Fig. 4(b), is similar to sample S1. The LMR starts to be observed in the optical spectrum at 3mm of immersion in water and at 5 mm the maximum depth is achieved. The same occurs for sample S3, Fig 4(c).

A first conclusion from the results obtained in Fig. 4 it is that in all cases the LMRs start to be observed after 3 mm of immersion. However, it must be highlighted that the L4 region is insensitive to refractive index because it presents no polishing. Therefore, in view that L4 region is around 1 mm, the minimum distance for generating an LMR subtracting L4 is around 1 mm, while the length required for attaining the maximum depths is around 3 mm, which is very interesting in applications such as probes with short sensing head. In addition, a clear difference is observed if we compare the results of S1 and S2 with respect to S3 in terms of FWHM in Fig. 5.

The S1 and S2 samples present a higher reduction of the FWHM as a function of the immersion in water than S3 sample. This is due to the placement of the fiber on the supporting platform during deposition process, which produces a gradient in the coating thickness along the fiber. There are some parameters that can affect the homogeneity of the deposition, mainly the angle, position and distance with respect to the target, and also to the optical properties of the specific materials.

The result is a widening of the LMR, which can be understood as the overlap of several resonances due to each of the different thickness values of the coating with gradient. As stated above, the position of the LMR is closely related to the coating thickness [3], which explains a broadening of the LMR when multiple thickness values exist in the same coating. As an example, the green plot in Fig. 4a, b and c is very smooth compared to the plots obtained after a higher immersion.

In order to support the previous idea, a theoretical analysis was performed for a 10 mm long D-shaped fiber in reflection configuration, which was coated with an SnO_{2-x} thin-film of thickness ranging from 125 to 185 nm The refractive could have gradient and depends on the deposition configuration from process to process. However, for the sake of simplicity we used a constant value of 1.9+0.01i based on ellipsometric measurements of [26]. The simulation tool used for the analysis was FIMMPROP, a module integrated with FIMMWAVE, and for the D-shaped region a finite-element method was used where 20 modes were analyzed.

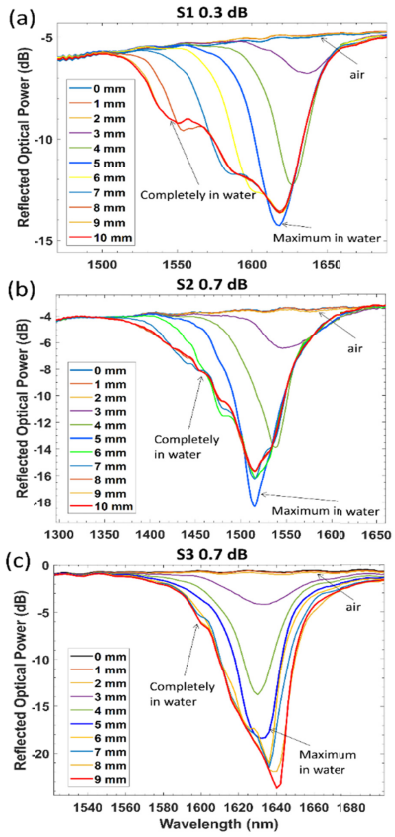

Fig 4: Reflection spectra corresponding to a progressive immersion in water, in steps of 1 mm for samples: (a) S1; (b) S2 and (c) S3.

The results in Fig. 6 show the optical spectra corresponding to 0 mm of immersion (all the device is surrounded by air), 1 mm of immersion (1 mm in water and 9 mm in air), 2 mm of immersion (2 mm in water and 8 mm in air) and so forth, up to 10 mm of immersion. The results show that the LMR is obtained at 1 mm of immersion and that a maximum depth is attained at 3 mm of immersion, corroborating the experimental results of Fig. 4. Here it must be pointed out that in the simulations there is an initial region of 1-2 mm (segment L4 in Fig. 2). Therefore, 1 to 3 mm corresponds with 2 to 4 mm or 3 to 5 mm in the experimental results. In addition, the experimental results of Fig. 5b also agree with the theoretical ones in terms of the stabilization of the LMR shape after 6-7 mm of immersion (in Fig. 6 this is achieved for 4 mm and it must be considered that in the simulations the L4 segment of 1-2 mm is not considered). A good agreement is also obtained with Fig. 5c, while this is not the case for Fig. 5a, probably because there is a higher gradient in the thin-film. The non-linear broadeding of the LMR obbeys to the fact that LMRs at short wavelengths are shallower than LMRs located at longer wavelengths [27]. Therefore, the contribution of the last part of D-shaped fiber immersed in water is less important than the first ones, where the coating is thicker.

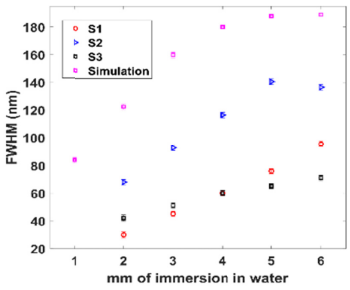

Fig 5. FWHM for different samples S1, S2, S3 and simulation.

The results observed with the different samples in Fig. 4 show that S2 is the sample with the worst performance in terms of FWHM. Consequently, it was decided to improve this parameter by removing part of its coating. In addition, due to the fact that when S2 was introduced in water the resonance reaches its best behavior at 5 mm of immersion, it was decided to begin the ablation process from the side of the fiber far from the tip, as described in Fig. 7 (a).

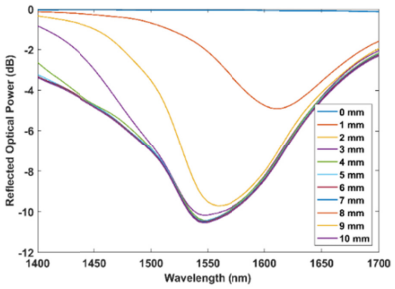

Fig 6: Theoretical results obtained with a D-shaped fiber coated with an SnO_{2-x} thin-film whose thickness ranges from 125 to 185 nm in a D-shaped region of 10 mm.

To this purpose, the SnO_{2-x} coating was removed gradually using a UV laser micromachining (OPTEC LB 1000, KrF, λ = 248 nm). Initially, 4 mm of coating were removed in 2 steps of 2 mm, then 2 mm in 2 steps of 1mm, one step of 0.5mm, and, finally, another step of 0.2 mm. Overall, 6.7 mm of the tin dioxide coating were removed. The final distance after laser cleaning from the tip of the fiber to the end of the SnO_{2-x} coating was 5.5 mm. This distance, corresponding with region A in Fig. 7(a), agrees with the 5 mm immersion length of the S2 sample where the most pronounced LMR peak was obtained in Fig. 4(b).

Fig. 7(b) shows the photograph with the coated and uncoated regions A and B, and Fig. 7(c) the effect of laser ablation on the optical spectrum respectively, can be distinguished. The existing resonances at shorter wavelengths were removed until there was only one narrow LMR whose -14dB losses has not been reduced and whose FWHM is 53 nm, which improves the 106 nm of the original sample (6.7 mm vs 0 mm uncoated in Fig. 7b). This demonstrates that it is possible to optimize the quality of the sample in terms of FWHM.

Finally, the sensitivity to RI was analyzed by using solutions with different concentration of ethanol in water. The results are shown in Fig 8. The RI of the solutions was obtained at a wavelength of 589 nm with a commercial refractometer Mettler Toledo® Refracto 30GS. The sensitivity was 6396 nm/RIU (see Fig. 8).

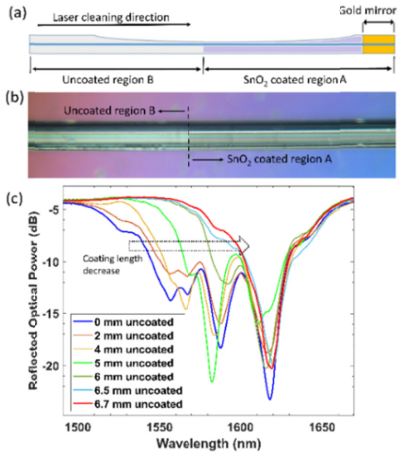

Fig 7: Cleaning of the S2 D-shaped with laser, (a) Schematic of the fibers with different regions: A and B, (b) spectra during cleaning, (c) image of the areas with deposition: region A, and clean: region B.

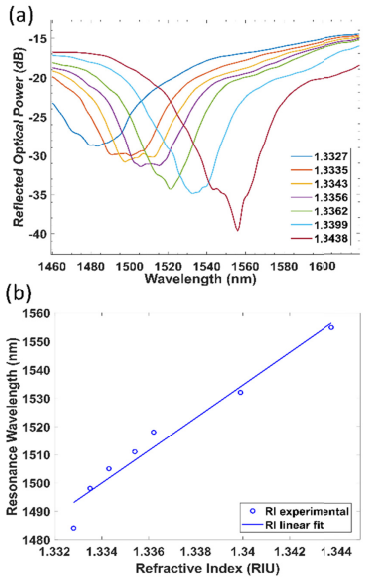

Fig 8: Response of S2 sample to different RI solutions: (a) Reflection spectra; (b) Wavelength shift as a function of RI.

To conclude, it has been demonstrated to be able to generate LMRs with thin-film coated D-shaped fiber in reflection configuration. In addition, it was observed that by a progressive immersion in water the FWHM of the structure can be optimized, which led to a further implementation using a laser ablation technique to confirm the ability to improve the FWHM by reducing the length of the coating. The non-optimal initial performance, before reducing the length of the coating, is attributed to the non-uniformity of the deposition, a presumption that was confirmed with simulations. In addition, using both methods, water immersion and laser ablation, it was observed that the optimal length of the coated region is 3 mm, which is really interesting in terms of using this structure with a short head in sensing applications. This method for optimizing the performance of LMRs obtained with thin-film coated D-shaped fiber can be used for applications such as chemical sensors or biosensors, where a low FWHM is critical for attaining a low limit of detection (LOD), and it can be applied for other domains such as the design of optical filters or resonators, just to mention a few.

Acknowledgment. Authors want to thank to the Government of Navarra for the International Mobility Aid 2019 and to the Spanish State Research Agency (AEI) for the funding through the projects TEC2016-79367-C2-2-R. Ministerio de Economía y Competitividad.

Disclosures. The authors declare no conflicts of interest.

References

1. E. Kretschmann, H. Raether, Zeitschrift für Naturforsch. 23, 2135, (1968).
2. J. Homola, M. Piliarik, Springer Ser Chem Sens Biosens 4, 45, (2006).
3. I. Del Villar, F. J. Arregui, C. R. Zamarreño, J. M. Corres, C. Bariáin, J. Goicoechea, C. Elosúa, M. Hernáez, P. J. Rivero, A. B. Socorro, A. Urrutia, P. Sánchez, P. Zubiate, D. López, N. De Acha, J. Ascorbe, I. R. Matías, Sens. Act. B Chem., 240, 174, (2017).
4. I. Del Villar, M. Hernáez, C. R. Zamarreño, P. Sanchez, C. Fernandez-Valdivielso, F. J. Arregui and I. R. Matías, Appl. Opt., 51, 19, 4298, (2012).
5. I. Del Villar, C. R. Zamarreño, M. Hernaez, P. Sanchez, F. J. Arregui, and I. R. Matias, Opt. Laser Technol. 69, 1, (2015).
6. S. P. Usha, A. M. Shrivastav, B. D. Gupta, Optical Fiber Technology, 45, 146, (2018).
7. M. Hernáez, I. Del Villar, C. R. Zamarreño, F. J. Arregui, and I. R. Matias, Appl. Opt., 49, 20, 3980, (2010).
8. C. R. Zamarreño, M. Hernáez, I. Del Villar, I. R. Matías, and F. J. Arregui, Sens. Actuators B, Chem., 155, 1, 290, (2011).
9. I. Del Villar, C. R. Zamarreño, P. Sanchez, M. Hernaez, C. F. Valdivielso, F. J. Arregui, and I. R. Matias, J. Opt. 12, 095503 (2010).
10. S. P. Usha, A. M. Shrivastav, B. D. Gupta, Biosensors and Bioelectronics, 87, 178, (2017).
11. A. B. Socorro, I. Del Villar, J. M. Corres, F. J. Arregui, I. R. Matias, IEEE Sens J, 12(8), 2598, (2012).
12. D. Tiwari, K. Mullaney, S. Korposh, S.W. James, S.-W. Lee, R.P. Tatam, Sens. Actuators B Chem. 242, 645, (2017).
13. M. Śmietana, M. Koba, P. Sezemsky, K. Szot-Karpińska, D. Burnat, V. Stranak, J. Niedziółka-Jönsson, R. Bogdanowicz, Biosensors and Bioelectronics, 154, (2020).
14. O. Fuentes, J.M. Corres, I.R. Matias, I. Del Villar, Journal of Lightwave Technology, 1, 99, (2019).
15. A. Andreev, B. Pantchev, P. Danesh, B. Zafirova, E. Karakoleva, E. Vlaikova, E. Alipieva, Sensors and Actuators B: Chemical, 106, 484, (2005).
16. F.J. Arregui, I. Del Villar, C.R. Zamarreño, P. Zubiate, I.R. Matias, Sensors and Actuators B: Chemical, 232, 660, (2016).
17. J. Arkwright, I. Underhill, S. Maunder, N. Blenman, M. Szczesniak, L. Wiklendt, I. Cook, D. Lubowski, and P. Dinning, Opt. Express, 17, 22423, (2009).
18. B. Carotenuto, A. Ricciardi, A. Micco, E. Amorizzo, M. Mercieri, A. Cutolo, A. Cusano, Sensors, 18, 2101, (2018).
19. P. Bechi, F. Pucciani, F. Baldini, et al. Digest Dis Sci 38, 1297, (1993).
20. P.R. Stoddart, D.J. White, Anal Bioanal Chem 394, 1761, (2009).
21. S Swarm, Vacuum, 38, 8, 791, (1988)
22. T. Wang, H. Yu, Z. Wu, Y. Jiang, J. Jiang, H. Jing, Proc SPIE, 7506. 10.1117, (2009).
23. F. Qi-hua, C. Xiao-hong, Z. Ying, Vacuum, 46, 3, 229, (1995).
24. A. Urrutia, I. Del Villar, P. Zubiate, C. R. Zamarreño, Laser & Photonics Reviews, 13, 1900094, (2019).
25. B. B. Sauer1, W. G. Kampert, Journal of Colloid and Interface Science, 199, 28, (1998).
26. F. Chiavaioli, P. Zubiate, I. Del Villar, C. R. Zamarreño, A. Giannetti, S. Tombelli, C. Trono, F. J. Arregui, I. R. Matias, F. Baldini, ACS Sensors 3(5), 936, (2018).
27. F. J. Arregui, I. Del Villar, C. R. Zamarreño, P. Zubiate, I. R. Matias, Sensors and Actuators B: Chemical, 232, 660, (2016).

References (extended version)

1. E. Kretschmann, H. Raether, “Radiative decay of nonradiative surface plasmons excited by light,” Zeitschrift für Naturforsch, 23, 2135-2136, (1968).

2. J. Homola, M. Piliarik, “Surface Plasmon Resonance (SPR) Sensors”, Springer Ser Chem Sens Biosens 4, 45-67, (2006).

3. I. Del Villar, F. J. Arregui, C. R. Zamarreño, J. M. Corres, C. Bariáin, J. Goicoechea, C. Elosúa, M. Hernáez, P. J. Rivero, A. B. Socorro, A. Urrutia, P. Sánchez, P. Zubiate, D. López, N. De Acha, J. Ascorbe, I. R. Matías, “Optical sensors based on lossy mode resonances,” Sens. Act. B Chem., 240, 174-185, (2017).

4. I. Del Villar, M. Hernáez, C. R. Zamarreño, P. Sanchez, C. Fernandez-Valdivielso, F. J. Arregui and I. R. Matías, “Design Rules for Lossy Mode Resonance Based Sensors,” Appl. Opt., 51, 19, 4298-4307, (2012).

5. I. Del Villar, C. R. Zamarreño, M. Hernaez, P. Sanchez, F. J. Arregui, and I. R. Matias, "Generation of Surface Plasmon Resonance and Lossy Mode Resonance by thermal treatment of ITO thin-films," Opt. Laser Technol. 69, 1-7, (2015).

6. S. P. Usha, A. M. Shrivastav, B. D. Gupta, “Semiconductor metal oxide/polymer based fiber optic lossy mode resonance sensors: A contemporary study,” Optical Fiber Technology, 45, 146-166, (2018).

7. M. Hernáez, I. Del Villar, C. R. Zamarreño, F. J. Arregui, and I. R. Matias, “Optical fiber refractometers based on lossy mode resonances supported by TiO 2 coatings,” Appl. Opt., 49, 20, 3980-3985, (2010).

8. C. R. Zamarreño, M. Hernáez, I. Del Villar, I. R. Matías, and F. J. Arregui, “Optical fiber pH sensor based on lossy-mode resonances by means of thin polymeric coatings,” Sens. Actuators B, Chem., 155, 1, 290-297, (2011).

9. I. Del Villar, C. R. Zamarreño, P. Sanchez, M. Hernaez, C. F. Valdivielso, F. J. Arregui, and I. R. Matias, "Generation of lossy mode resonances by deposition of high-refractive-index coatings on uncladded multimode optical fibers," J. Opt. 12, 095503 (2010).

10. S. P. Usha, A. M. Shrivastav, B. D. Gupta, “A contemporary approach for design and characterization of fiber-optic-cortisol sensor tailoring LMR and ZnO/PPY molecularly imprinted film,” Biosensors and Bioelectronics, 87, 178-186, (2017).

11. A. B. Socorro, I. Del Villar, J. M. Corres, F. J. Arregui, I. R. Matias, “Tapered single-mode optical fiber pH sensor based on lossy mode resonances generated by a polymeric thin-film,” IEEE Sens J, 12(8), 2598-2603, (2012).

12. D. Tiwari, K. Mullaney, S. Korposh, S.W. James, S.-W. Lee, R.P. Tatam, “An ammonia sensor based on Lossy Mode Resonances on a tapered optical fibre coated with porphyrin-incorporated titanium dioxide,” Sens. Actuators B Chem. 242, 645-652, (2017).

13. M. Śmietana, M. Koba, P. Sezemsky, K. Szot-Karpińska, D. Burnat, V. Stranak, J. Niedziółka-Jönsson, R. Bogdanowicz, “Simultaneous optical and electrochemical label-free biosensing with ITO-coated lossy-mode resonance sensor,” Biosensors and Bioelectronics, 154, (2020).

14. O. Fuentes, J.M. Corres, I.R. Matias, I. Del Villar, “Generation of Lossy Mode Resonances in Planar Waveguides Toward Development of Humidity Sensors,” Journal of Lightwave Technology, 1, 99, (2019).

15. A. Andreev, B. Pantchev, P. Danesh, B. Zafirova, E. Karakoleva, E. Vlaikova, E. Alipieva, “A refractometric sensor using index-sensitive mode resonance between single-mode fiber and thin film amorphous silicon waveguide,” Sensors and Actuators B: Chemical, 106, 484-488, (2005).

16. F.J. Arregui, I. Del Villar, C.R. Zamarreño, P. Zubiate, I.R. Matias, “Giant sensitivity of optical fiber sensors by means of lossy mode resonance,” Sensors and Actuators B: Chemical, 232, 660-665, (2016).

17. J. Arkwright, I. Underhill, S. Maunder, N. Blenman, M. Szczesniak, L. Wiklendt, I. Cook, D. Lubowski, and P. Dinning, "Design of a high-sensor count fibre optic manometry catheter for in-vivo colonic diagnostics," Opt. Express, 17, 22423-22431, (2009).

18. B. Carotenuto, A. Ricciardi, A. Micco, E. Amorizzo, M. Mercieri, A. Cutolo, A. Cusano, “Smart Optical Catheters for Epidurals,” Sensors, 18, 2101, (2018).

19. P. Bechi, F. Pucciani, F. Baldini, et al. “Long-term ambulatory enterogastric reflux monitoring,” Digest Dis Sci 38, 1297-1306, (1993).

20. P.R. Stoddart, D.J. White, “Optical fibre SERS sensors,” Anal Bioanal Chem 394, 1761-1774, (2009).

21. S Swarm, “Film thickness distribution in magnetron sputtering,” Vacuum, 38, 8 - 10, 791 – 794, (1988)

22. T. Wang, H. Yu, Z. Wu, Y. Jiang, J. Jiang, H. Jing, “Analysis of film thickness for magnetron sputtering system with more than one workbench,” Proc SPIE, 7506. 10.1117, (2009).

23. F. Qi-hua, C. Xiao-hong, Z. Ying, “Computer simulation of film thickness distribution in symmetrical magnet magnetron sputtering,” Vacuum, 46, 3, 229-232, (1995).

24. A. Urrutia, I. Del Villar, P. Zubiate, C. R. Zamarreño, “A Comprehensive Review of Optical Fiber Refractometers: Toward a Standard Comparative Criterion,” Laser & Photonics Reviews, 13, 1900094, (2019).

25. B. B. Sauer, W. G. Kampert, “Influence of Viscosity on Forced and Spontaneous Spreading: Wilhelmy Fiber Studies Including Practical Methods for Rapid Viscosity Measurement," Journal of Colloid and Interface Science, 199, 1, 28-37, (1998).

26. F. Chiavaioli, P. Zubiate, I. Del Villar, C. R. Zamarreño, A. Giannetti, S. Tombelli, C. Trono, F. J. Arregui, I. R. Matias, F. Baldini, “Femtomolar Detection by Nanocoated Fiber Label-Free Biosensors,” ACS Sensors 3(5), 936-943, (2018).

27. F. J. Arregui, I. Del Villar, C. R. Zamarreño, P. Zubiate, I. R. Matias, “Giant sensitivity of optical fiber sensors by means of lossy mode resonance,” Sensors and Actuators B: Chemical, 232, 660-665, (2016).